Mon. Not. R. Astron. Soc. **000**, 000–000 (0000) Printed 22 March 2009 (MN LATEX style file v2.2)

Expected high energy emission from GRB 080319B and origins of the GeV emission of GRBs 080514B, 080916C and 081024B

Yuan-Chuan Zou[1,3], Yi-Zhong Fan[2,4], and Tsvi Piran[1] ⋆
[1]*The Racah Institute of Physics, Hebrew University, Jerusalem 91904, Israel*
[2]*Niels Bohr International Academy, Niels Bohr Institute, University of Copenhagen, Blegdamsvej 17, DK-2100 Copenhagen, Denmark*
[3]*School of Physics, Huazhong University of Science and Technology, 430074, Wuhan, China*
[4]*Purple Mountain Observatory, Chinese Academy of Sciences, Nanjing 210008, China*

22 March 2009

ABSTRACT
We calculate the high energy (sub-GeV to TeV) prompt and afterglow emission of GRB 080319B that was distinguished by a naked-eye optical flash and by an unusual strong early X-ray afterglow. There are three possible sources for high energy emission: the prompt optical and γ-ray photons IC scattered by the internal shock electrons, the prompt photons IC scattered by the early external reverse-forward shock electrons, and the higher band of the synchrotron and the synchrotron self-Compton emission of the external shock. There should have been in total ~ 500 high energy photons detectable for the Large Area Telescope (LAT) onboard the Fermi satellite, and > 30 photons of those with energy > 10 GeV. The > 10 GeV emission had a duration about twice that of the soft γ-rays. AGILE could have observed these energetic signals if it was not occulted by the Earth at that moment. The physical origins of the high energy emission detected in GRB 080514B, GRB 080916C and GRB 081024B are also discussed. These observations can be reasonably interpreted by available high energy emission models based on our current understanding of GRBs and afterglows.

Key words: gamma rays: bursts−radiation mechanism: nonthermal

1 INTRODUCTION

A breakthrough of GRB observation, made by *Swift* satellite in 2008, is the discovery of the very bright burst GRB 080319B which was accompanied by a naked-eye optical flash (Racusin et al. 2008b). The optical observation was going on even before the onset of the γ-ray burst because TORTORA was monitoring the same region of the sky at that moment (Cwiok et al. 2008; Karpov et al. 2008). The X-ray telescope (XRT) onboard *Swift* satellite slewed to the source about 60 sec after the trigger of the burst and recorded a quickly decaying but extremely bright X-ray component. These continuous observations collected fruitful data (Racusin et al. 2008b; Bloom et al. 2008) and rendered GRB 080319B one of the best-studied bursts so far. Although no very high-energy emission was directly detected from GRB 080319B the unique spectrum of this burst and its afterglow suggest that it has been accompanied by a very strong GeV-TeV emission that would have already been detected by AGILE if not occulted by earth at that moment. Based on a model in which the prompt optical and soft γ-ray emission are respectively the synchrotron and the first order inverse Compton (IC) radiation components of the internal shocks, Kumar & Panaitescu (2008), Racusin et al. (2008) and Fan & Piran (2008) suggested that the second order IC of the internal shocks would peak in GeV-TeV energy range and the isotropic energy might be high up to $\sim 10^{55}$ erg (see however Piran, Sari & Zou 2008). Because of the tight overlapping of the prompt emission with the reverse/forward shock regions, some soft γ-rays will be up-scattered by the reverse shock electrons and some prompt optical photons will be up-scattered by the forward shock electrons, i.e., the so-called external inverse Compton (EIC). As a result, two additional GeV-TeV emission components with a duration ~ 100 s are expected (Fan & Piran 2008). In this work, we discuss these possibilities in more detail. Moreover, we show that the early $(60 - 2000$ s) forward shock synchrotron and the synchrotron self-Compton (SSC) emission in the energy range $20\mathrm{MeV} - 300\mathrm{GeV}$ is as powerful as the high energy emission detected in GRB 080916C (Tajima et al. 2008). A schematic plot of the expected GeV-TeV signals from GRB 080319B is shown in Fig.1.

Since its successful launch on June 11 2008, the Fermi satellite has detected the prompt > 10 GeV emission in GRB 080916C (Tajima et al. 2008; Omodei 2008), and the GeV emission following a short burst GRB 081024B (Omodei et al. 2008). As GRB 080514B (Giuliani et al. 2008), GRB 080825C (Bouvier et al. 2008), and some other events detected by the Compton Gamma Ray Observatory (CGRO) satellite in 1991-2000 (Hurley et al. 1994; González et al. 2003), the high energy emission of both GRB 080916C and GRB 081024B lasted longer than the prompt soft γ-rays. The detection of high energy signals sheds some lights on

⋆ Email: yizhong@nbi.dk (YZF) and tsvi@phys.huji.ac.il (TP)

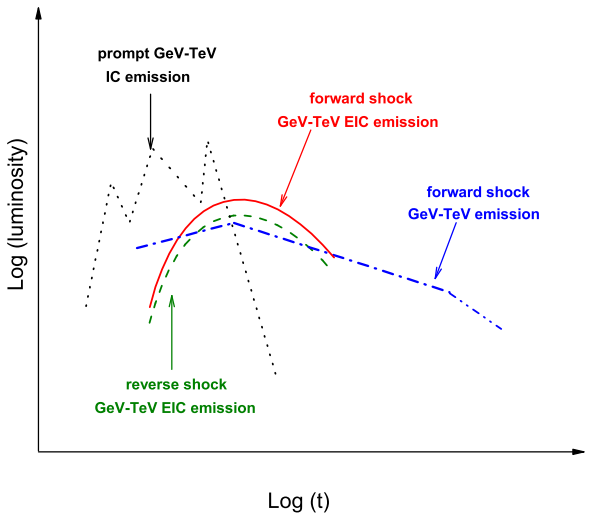

Figure 1. Schematic light curves for the different component of the high energy emissions: internal shocks SSC, reverse shock EIC, forward shock EIC and external shock SSC respectively.

the bulk Lorentz factor of the ejecta, the radiation mechanisms, the physical composition of the outflow and the prolonged activity of the central engine. This is particularly the case if the simultaneous X-ray/optical emission data are available (see Fan & Piran 2008 for a recent review). In this work we'll outline the origins of the GeV emission from GRB 080514B, GRB 080916C and GRB 081024B, based on the (preliminary) public data.

The paper is structured as follows. In Section 2, we calculate the possible prompt and afterglow GeV-TeV emission of GRB 080319B. In section 3, we interpret the high energy emission detected in GRB 080514B, GRB 080916C and GRB 081024B. In section 4, we summarize our results with some discussions.

2 POSSIBLE GEV-TEV EMISSION FROM GRB 080319B

GRB 080319B (Racusin et al. 2008b) was most notable due to its huge total energy and especially its extremely luminous prompt optical emission that could be seen with naked eyes (Cwiok et al. 2008; Karpov et al. 2008). This burst was located at a redshift $z = 0.937$ space (Vreeswijk et al. 2008) and duration was T_{90} ∼57s. The peak energy of the νF_ν spectrum was $E_{\rm p} \simeq 675 \pm 22$ keV, and the photon indexes below and above E_p were $-0.855^{+0.014}_{-0.013}$ and $-3.59^{+0.32}_{-0.62}$ respectively. Choosing standard cosmological parameters $H_0 = 70{\rm km\,s^{-1}\,Mpc^{-1}}, \Omega_{\rm M} = 0.3, \Omega_\Lambda = 0.7$(corresponding to a luminosity distance $D_L \sim 1.9\times 10^{28}$cm), we have a peak luminosity $L_{\rm peak} \sim 1.0 \times 10^{53}{\rm erg}\,s^{-1}$ and an isotropic energy $E_{\rm iso} \simeq 1.3 \times 10^{54}$ erg (Racusin et al. 2008b; Bloom et al. 2008; Golenetskii et al. 2008). Karpov et al. (2008) reported the optical V-band ($\sim 6 \times 10^{14}$Hz) light curve in the prompt phase (from ∼ -10 s to ∼ 100 s). Variability was evident and there were at least 3 or 4 main pulses in the light curve. The peak V-band reached magnitude of 5.3, corresponding to a flux density ∼ 28.7 Jy, and energy $E_{opt} \sim 2\times 10^{52}$erg if we take ∼ 20 Jy as the average flux density. The variability and the very sharp decline of the prompt optical emission support an internal origin of these optical photons, though the underlying physical process is not clear yet (see Zou, Piran & Sari 2008, for a discussion of various possible models).

Afterglow modeling can in principle constrain the total kinetic energy and the initial Lorentz factor of the GRB ejecta, and the physical parameters of the external shocks (Sari, Piran & Narayan 1998; Chevalier & Li 2000; Panaitescu & Kumar 2001). The behavior of the afterglow of GRB 080319B suggests a free wind medium (Kumar & Panaitescu 2008; Racusin et al. 2008; Wu et al. 2008). A self-consistent modeling of the X-ray and optical afterglow data favors a two-component jet model (Racusin et al. 2008; Wu et al. 2008). Moreover, the shock parameters of the narrow and wide ejecta components need to be very different, as found in GRB 051221A (Jin et al. 2007). Following Racusin et al. (2008) and Wu et al. (2008), we take the isotropic kinetic energy of the narrow ejecta (represented by the subscript "n") $E_{\rm k,n} \sim 3\times 10^{55}$ erg[1], the wind parameter $A_* \sim 0.01$, the fraction of forward shock energy given to the electrons $\epsilon_{\rm e,n} \sim 0.1$, the fraction of forward shock energy given to the magnetic field[2] $\epsilon_{\rm B,n} \sim 10^{-4}$, the power-law distribution index $p_{\rm n} \sim 2.4$, and the half-opening angle $\theta_{\rm j,n} \sim 0.2$ degree. We do not discuss the wide jet component because it plays a less important role in producing GeV-TeV afterglow emission. The average Lorentz factor of the narrow jet outflow ($\Gamma_{\rm i}$) before getting decelerated by a stellar wind medium is very high. A lower limit can be set by the Lorentz factor of the forward shock at ∼ 70 s, when the X-ray afterglow began to decline normally, i.e. (Blandford & McKee 1976; Dai & Lu 1998),

$$\Gamma \simeq 600 E_{\rm k,n,55.5}^{1/4} A_{*,-2}^{-1/4} (t/70{\rm s})^{-1/4} [(1+z)/2]^{1/4}.$$

So a choice of $\Gamma_{\rm i} \sim 1000$ is rather reasonable. Throughout this work we adopt the convenience $Q_{\rm x} = Q/10^{\rm x}$ in units of cgs

In the leading fireball model for GRBs (see Piran 2004; Mészáros 2002; Zhang 2007, for reviews), the synchrotron and IC radiation will give rise to a high-energy component that will be emitted along with the prompt sub-MeV photons and the afterglow radio/optical/X-ray emission (Fan & Piran 2008). Depending on the seed photons' origins, IC can be SSC or EIC. Below we'll show that for GRB 080319B both processes plausibly played an important role in producing GeV−TeV emission. This suggests that similar bursts will provide promising sources for the Fermi high energy satellite.

[1] An $E_{\rm k,n}$ high up to $\sim 10^{55}$ erg is rather unusual. Similar result has only been reported in the afterglow modeling of GRB 060418 (Jin & Fan 2007). However we believe that such a huge value is possible for GRB 0980319B because the XRT flux at $t \sim 70$ s is as bright as $\sim 10^{-7}$ erg s^{-1} cm^{-2}, which is the strongest X-ray afterglow detected so far and is even much brighter than most prompt X-ray emission of *Swift* GRBs. On the other hand both the spectral and the temporal behaviors of the early ($60 - 2000$ s) X-ray emission strongly favor a fireball model in the slow cooling phase, which requires small $\epsilon_{\rm B,n}$ and A_*. As a result, we do need an $E_{\rm k,n} \sim 10^{55}$ erg to reproduce the observation data (see footnote 2).

[2] We do not take $\epsilon_{\rm n,B} \sim 10^{-6}$ as in Racusin et al. (2008) (see section 2.2 below) because the peak flux density of the forward shock synchrotron emission is $F_{\nu,\rm max}^{\rm syn} \sim 9\epsilon_{\rm B,n,-4}^{1/2} E_{\rm k,n,55.5}^{1/2} A_{\star,-2} D_{L,28.3}^{-2} t_3^{-1/2}$mJy. At $t \sim 60$ sec, the X-ray (at 1 keV) flux ∼ 20 mJy (Bloom et al. 2008) disfavors an $\epsilon_{\rm B,n}$ as small as $\sim 10^{-6}$. On the other hand, an $\epsilon_{\rm B,n} \sim 10^{-6}$ will give rise to a too large cooling Lorentz factor $\gamma_{\rm c} \sim 10^{10}(1+Y_{\rm ssc})^{-1}$, where the forward shock SSC parameter $Y_{\rm ssc} \ll \sqrt{\epsilon_{\rm n,e}/\epsilon_{\rm B,n}}$ since the SSC emission of such energetic electrons should be in Klein-Nishina regime and thus be effectively suppressed.

2.1 Prompt GeV-TeV IC emission

Zou, Piran & Sari (2008) showed that the SSC models in which the soft γ-rays are the CI of the optical photons cannot explain the observations. The major obstacle is the resulting high synchrotron self-absorption frequency and then the X-ray spectrum that is inconsistent with the observation. If we ignore this problem, there is a solution with a Compton parameter $Y \sim 1$ and a stochastic Lorentz factor $\gamma_{\rm e} \sim 100$. Then the 2nd IC peaks at $2\gamma_{\rm e}^2 E_{\rm p} \sim 15$ GeV, and the number of the detectable photons is $YE_\gamma S_{\rm det}/4\pi D_L^2 h\nu_{\rm 2nd,IC}$ corresponding to detected ~ 130 photons by LAT, with $S_{\rm det} \sim 10^4{\rm cm}^2$ at GeV energies. Other models with larger Y lead to even stronger signals (Kumar & Panaitescu 2008; Racusin et al. 2008).

Below we consider the possibility (Zou, Piran & Sari 2008) that the prompt optical photons and the soft γ-rays of GRB 080319B arose from two different regions, denoted by the subscripts "opt" and "γ" respectively. Strong high energy prompt emission is still possible, and it can be estimated even though the physical origin of the prompt emission is still unclear. The possible high energy emission consists of four components: self-IC scattering in the optical emission region; self-IC scattering in the γ-ray producing region; optical photons IC scattered in the γ-ray producing region; and soft γ-rays IC scattered in the optical emission region. Note that because of the steep decline of the high energy slope ($\beta \sim 2.6$) extropolation of the soft γ-ray emission gives only a very weak signal.

2.1.1 Prompt optical emission region

The observed optical flux density limits the temperature of this region:

$$f_{\nu,\rm opt} \leqslant \frac{2\pi[\nu_{\rm opt}(1+z)]^2\Gamma_{\rm opt}kT_{\rm opt}}{c^2}\left(\frac{R_{\rm opt}}{\Gamma_{\rm opt}D_L}\right)^2, \quad (1)$$

where $\Gamma_{\rm opt}$ is the bulk Lorentz factor, k is Boltzmann constant, $T_{\rm opt}$ is the temperature (while the minimal temperature $T_{\rm opt,min}$ corresponds to the equality), and $R_{\rm opt}$ is the emission region radius. Thus

$$kT_{\rm opt,min} = 1.2\times10^{-4}\Gamma_{\rm opt,3}R_{\rm opt,16}^{-2}\ {\rm erg}. \quad (2)$$

Noticing that the bulk Lorentz factor in the afterglow is high (Racusin et al. 2008), we take a fiducial value of $\Gamma_{opt} \sim 10^3$ for the prompt phase. Considering the variability of the light curves and the deceleration radius, which constrains the radius should not be too large, then the choice 10^{16}cm is reasonable. The corresponding typical stochastic Lorentz factor of the electrons is

$$\gamma_{\rm e,opt,min} \sim kT_{\rm opt,min}/(m_{\rm e}c^2) \sim 150\Gamma_{\rm opt,3}R_{\rm opt,16}^{-2}, \quad (3)$$

where $m_{\rm e}$ is the rest mass of the electron.

The first order IC is in the soft γ-ray band. As mentioned before the prompt soft γ-rays are unlikely to be the first order IC component of the optical emission. So the first order IC radiation of the electrons emitting optical photons would be much smaller than the detected soft γ-rays. Correspondingly, the 2nd order IC radiation in GeV-TeV energy range is unimportant as it falls below the IC radiation that arises when the prompt soft γ-rays cross the optical emission region.

2.1.2 γ-rays IC scattered in the prompt optical emission region

If the soft γ-rays pass through the prompt optical emitting electrons, the "optical depth" for electrons is approximately $\sigma_T\frac{N_\gamma\delta t_{\rm opt}/T_{90}}{4\pi R^2} \sim 3N_{\gamma,60}R_{16}^{-2}\delta t_{\rm opt,-0.5}$, where $\delta t_{\rm opt} \sim 0.3\ R_{\rm opt,16}\Gamma_{\rm opt,3}^{-2}$s is the typical variability timescale of the prompt optical emission. For each collision the electron loses energy $\sim \gamma_{\rm e,opt}^2 h\nu_\gamma/\Gamma_{\rm opt} < \gamma_{\rm e,opt}m_ec^2$ as long as $\gamma_{\rm e,opt} < \Gamma_{\rm opt}$.

Assuming that almost all electrons carried by the GRB outflow contributed to the prompt optical emission, which should be an upper limit, we estimate the number of electrons that participate in a typical optical pulse (with a variability timescale $\delta t_{\rm opt}$):

$$N_{\rm e,p,opt} \sim \frac{E_{\rm k,n}\delta t_{\rm opt}}{\Gamma_{\rm i}m_{\rm p}c^2T_{90}} \sim 10^{53}E_{\rm k,n,55.5}\delta t_{\rm opt,-0.5}\Gamma_{\rm i,3}^{-1}. \quad (4)$$

Using this value we estimate the optical depth for soft $\gamma-$rays being scattered by the electrons emitting the prompt optical emission as $\tau \sim \sigma_{\rm T}N_{\rm e,p,opt}/(4\pi R_{\rm opt}^2) \sim 5\times10^{-5}E_{\rm k,n,55.5}\delta t_{\rm opt,-0.5}\Gamma_{\rm i,3}^{-1}R_{\rm opt,16}^{-2}$. The total number of the IC photons detectable by LAT is thus

$$N_{{\rm det},\gamma-{\rm opt}} \sim \frac{\tau N_\gamma S_{\rm det}}{4\pi d_L^2} \leqslant 100E_{\rm k,n,55.5}\delta t_{\rm opt,-0.5}\Gamma_{\rm i,3}^{-1}R_{\rm opt,16}^{-2}N_{\gamma,60}, \quad (5)$$

where N_γ is the total number of prompt soft $\gamma-$rays. The typical energy of the IC photons is greater than $E_{{\rm IC},\gamma-{\rm opt}} \sim 2\gamma_{\rm e,opt,min}^2E_p \sim 30\Gamma_{\rm opt,3}^2R_{\rm opt,16}^{-4}$ GeV. The corresponding total energy of these photons is $\sim 2\times10^{54}$ergs.

2.1.3 Soft γ-ray emission region

Since there may be no suitable IC model for the soft γ-rays, we assume that these soft γ-rays are the synchrotron emission of the internal shocks at a radius R_γ. To match the peculiar spectrum of the soft γ-rays, the cooling Lorentz factor $\gamma_{\rm c} \sim (1+z)\frac{6\pi m_ec}{\sigma_{\rm T}\Gamma B^2\delta t_\gamma}$ should be comparable to the typical Lorentz factor of the electrons $\gamma_{\rm m}$ (Zou, Piran & Sari 2008). $\sigma_{\rm T}$ is the Thompson's cross section and $\delta t_\gamma \sim 0.1$s (Margutti et al. 2008) is the variability timescale of the soft γ-rays. The condition $E_{\rm p} \sim \Gamma_\gamma 2\gamma_{e,\gamma}^2\frac{q_{\rm e}B_\gamma}{m_{\rm e}c}/(1+z)$ gives

$$B_\gamma \sim 16\Gamma_{\gamma,3}^{-1/3}\delta t_{\gamma,-1}^{-2/3}{\rm Gauss}, \quad (6)$$

where $q_{\rm e}$ is the electron's charge. The typical Lorentz factor of the emitting electrons is thus

$$\gamma_{{\rm e},\gamma} \sim 6\times10^4\Gamma_{\gamma,3}^{-1/3}\delta t_{\gamma,-1}^{1/3}. \quad (7)$$

The SSC will be deep in the Klein-Nishina regime, and pair avalanche effect might exist (Piran, Sari & Zou 2008), additional component of high energy photons would peak at energy $\Gamma_\gamma^2(m_ec^2)^2/(h\nu_\gamma) \sim 400\Gamma_{\gamma,3}^2$ GeV, where h is the Plank constant.

Using $f_{\nu,\rm max} = (1+z)N_{{\rm e},\gamma}\Gamma_\gamma m_{\rm e}c^2\frac{\sigma_{\rm T}B}{3q_{\rm e}4\pi D_L^2}$, we get the number of electrons for each pulse $N_{\rm e,p,\gamma} \sim 9\times10^{49}\Gamma_{\gamma,3}^{-2/3}\delta t_{\gamma,-1}^{2/3}$, and the total number of electrons is then $N_{{\rm e},\gamma} \sim N_{\rm e,p,\gamma}T_{90}/\delta t_\gamma \sim 5\times10^{52}\Gamma_{\gamma,3}^{-2/3}\delta t_{\gamma,-1}^{-1/3}$.

The corresponding optical depth for Thompson scattering is $\tau \sim \sigma_T N_{{\rm e},\gamma}/(4\pi R_\gamma^2) \sim 5\times10^{-8}N_{\rm e,p,\gamma,50}R_{\gamma,16}^{-2}$. [3] And the Compton parameter in KN regime is $Y \sim \gamma_{e,\gamma}^2\tau/[\gamma_{e,\gamma}h\nu_\gamma/(\Gamma m_ec^2)]^2 \sim 0.03\Gamma_{\gamma,3}^2N_{\rm e,p,\gamma,50}R_{\gamma,16}^{-2}$(Piran, Sari & Zou 2008). The total energy of the avalanche loaded pairs is in the order of $2YE_\gamma$

[3] By the time a single photon passes through a sub-shell, this sub-shell expands by a factor of $\sim$2 in radius. Therefore subsequent scattering in other sub-shells will be negligible and when considering the optical depth a single sub-shell should be taken into account.

even all the first produced very high energy photons are cooled into steady pairs. The number of detectable photons by LAT is then $\sim 0.1 R_{\gamma,16}^{-2}$. It is thus undetectable even without taking into account the large optical depth ($\sim$ 10) of the universe to such energetic photons (Stecker et al. 2006).

2.1.4 optical photons IC scattered in γ-rays region

If the optical photons are produced in smaller radii than the soft γ-rays ($R_\gamma \geqslant R_{\rm opt}$), they would be IC scattered in the γ-rays region. In this case, the electrons will be cooled to a random Lorentz factor $\gamma_{\rm e,\gamma,c} < 1.8\times10^4 \Gamma_{\gamma,3}^3 R_{\gamma,16} L_{\rm opt,50.7}^{-1} < \gamma_{\rm e,\gamma}$ (Fan & Piran 2008), where $L_{\rm opt} > 5\times10^{50}{\rm erg\,s^{-1}}$ is the luminosity of the prompt optical emission, suggesting that all the electrons were cooled by the IC scattering. The typical energy of the IC scattered photons is $E_{\rm IC,opt-\gamma} \sim 2\gamma_{\rm e,\gamma}^2 h\nu_{opt} \sim 14\Gamma_{\gamma,3}^{-2/3}\delta t_{\gamma,-1}^{2/3}$GeV. Since the electrons lost almost all the energy, the number of the detectable photons by LAT is

$$N_{\rm det,opt-\gamma} \sim \frac{E_{\rm e,\gamma} S_{\rm det}}{4\pi D_L^2 E_{\rm IC,opt-\gamma}} \sim 240 \Gamma_{\gamma,3}^{-1/3} \delta t_{\gamma,-1}^{-2/3} \quad (8)$$

where $E_{\rm e,\gamma} \approx \Gamma_\gamma \gamma_{\rm e,\gamma} N_{\rm e,\gamma} m_{\rm e} c^2$ is the total energy carried by the electrons emitting soft $\gamma-$rays.

This discussion is valid only for $R_\gamma \geqslant R_{\rm opt}$. As long as $R_{\rm opt} \gtrsim$ a few$\times R_\gamma$, the prompt optical emission cannot cool the internal shock electrons emitting soft $\gamma-$rays, because the photons from $R_{\rm opt}$ reached R_γ in a time $\sim (R_{\rm opt}-R_\gamma)/c \sim 3\times10^5\ R_{\rm opt,16}$ sec when the internal shocks at R_γ had disappeared long before. For the same reason, there would be no high energy photons produced by the optical region electrons as presented in section 2.1.2 (i.e., $N_{\rm det,\gamma-opt}=0$) if $R_\gamma > R_{\rm opt}$.

2.2 Very early EIC emission

Whatever the mechanism is, the prompt emission should have an internal origin, in view of the high variability of the light curves and the very sharp decline at $t > T_{90}$. External reverse-forward shock formed very quickly. Consequently, the prompt photons passing though the reverse/forward shock regions were IC scattered by the shock accelerated electrons. As a result, two additional GeV-TeV EIC components were present.

2.2.1 EIC in reverse shock region

Racusin et al. (2008) and Wu et al. (2008) argued that the reverse shock emission of the narrow jet component had not been seen. Its physical parameters are thus unknown. We simply assume that they are the same as those of the forward shock.

The reverse shock emission must have overlapped the prompt gamma-rays and optical emission. Therefore the electrons accelerated by the reverse shock front were cooled by the prompt emission and gave rise to an EIC radiation component (Beloborodov 2005; Fan, Zhang & Wei 2005).

The number of electrons in the reverse shock region is

$$N_{\rm e,r} \simeq \frac{E_{\rm k,n}}{\Gamma m_p c^2} \simeq 3\times10^{55} E_{\rm k,n,55.5} \Gamma_{2.8}^{-1}. \quad (9)$$

The typical radius of the reverse shock can be estimated as

$$R_{\rm r} \sim 2\Gamma^2 c T_{90}/(1+z) \sim 5\times10^{17}\Gamma_{2.8}^2\ {\rm cm}. \quad (10)$$

The optical depth of the prompt photons being scattered by the electrons was

$$\tau_{\rm r} \sim \sigma_{\rm T} \frac{N_{\rm e,r}}{4\pi R_{\rm r}^2} \sim 7\times10^{-6} E_{\rm k,n,55.5} \Gamma_{2.8}^{-1} R_{17.7}^{-2}. \quad (11)$$

On the other hand, the total number of the prompt soft γ-rays that reached us (per area) can be estimated as (Fan & Piran 2006)

$$N_{\rm tot,\gamma} \sim \frac{\beta_\gamma - 1}{\beta_\gamma} \frac{\mathcal{F}}{h\nu_{\gamma,\rm p}}, \quad (12)$$

where $\mathcal{F} \sim 10^{-4}\ {\rm erg\ cm^{-2}}$ is the energy fluence of the prompt γ-rays and $\beta_\gamma \sim 2.6$ is the high energy spectral index of the prompt γ-ray emission.

The number of the reverse shock EIC photons detectable by the Fermi satellite and their typical energy can be estimated as

$$N_{\rm det,r} \sim \tau_{\rm r} N_{\rm tot,\gamma} S_{\rm det} \sim 3, \quad (13)$$

and

$$h\nu_{\rm EIC,r} \sim 2\gamma_{\rm m,r}^2 E_{\rm p} \sim 13\ {\rm GeV}\ (\frac{\gamma_{\rm m,r}}{100})^2, \quad (14)$$

where $\gamma_{\rm m,r}$ [4] is the minimal Lorentz factor of the electrons accelerated in the reverse shock front. The electrons are in slow cooling phase since the cooling Lorentz factor is (Fan & Piran 2008)

$$\gamma_{\rm c,r} \sim 10^3 \Gamma_{2.8}^3 R_{\rm r,17.7} L_{\gamma,52.7}^{-1} > \gamma_{\rm m,r}. \quad (15)$$

The Compton parameter $Y_{\rm EIC,r} \sim \gamma_{\rm m,r}^2 \tau_{\rm r} \ll 1$. So the energy of this EIC component was much smaller than that of the prompt soft γ-rays.

Here we do not take into account the cooling caused by the synchrotron radiation because $U_B \sim \varepsilon_B 4\Gamma^2 A R^{-2} m_p c^2 \sim 3.3\times10^{-3}\varepsilon_{\rm n,B,-4}\Gamma_{2.8}^2 A_{\star,-2} R_{17.7}^{-2} {\rm erg\,cm^{-3}}$, which is much smaller than $U_\gamma \sim \frac{L_\gamma}{4\pi R^2\Gamma^2 c} \sim 1.3\Gamma_{2.8}^{-2} R_{17.7}^{-2} {\rm erg\,cm^{-3}}$.

Some prompt optical photons will be up-scattered by the reverse shock electrons and will be boosted to an energy $\sim 2\gamma_{m,r}^2 h\nu_{\rm opt} \sim 10$ keV, which is too low to be of interest.

2.2.2 EIC in forward shock region

The prompt emission will cool the forward shock electrons as well (Fan, Zhang & Wei 2005; Wang & Mészáros 2006). However, for the prompt γ-rays, this EIC process is unimportant since it is in the Klein-Nishina regime. Because the large radius lowers the optical depth, pair avalanche does not exist in this case. Here we focus on the EIC radiation of the prompt optical emission. The energy density of the emitted prompt photons is $U_{\rm opt} \sim \frac{L_{\rm opt}}{4\pi R^2\Gamma^2 c} \sim 0.05\ L_{\rm opt,51}\Gamma_{2.8}^{-2} R_{17.7}^{-2} {\rm erg\,cm^{-3}}$, which is larger than $U_{\rm B}$. So the cooling of the forward shock electrons is dominated by the EIC process.

The number of the electrons swept by the forward shock is

$$N_{\rm e,f} \simeq 4\pi A R \simeq 1.8\times10^{52} A_{\star,-2} R_{17.7}. \quad (16)$$

The optical depth of the prompt photons for being scattered is thus

$$\tau_{\rm f} \sim \sigma_{\rm T} \frac{N_{\rm e,f}}{4\pi R^2} \sim 3\times10^{-9} A_{\star,-2} R_{17.7}^{-1}. \quad (17)$$

Noticing that we don't know the spectrum in the optical band,

[4] $\gamma_{\rm m,r} \sim \epsilon_{\rm e,n}(\bar\gamma-1) m_{\rm p}/m_{\rm e}(p_{\rm n}-2)/(p_{\rm n}-1)$, where $m_{\rm p}$ is the rest mass of the protons, and $\bar\gamma$ indicates the internal energy density in the shocked region. For the mildly Relativistic reverse shock we have $\bar\gamma - 1 \sim 1$ (see Zou, Wu & Dai 2005, for details), which is the case for this burst.

the total number of the optical photons reaching us (in unit area) can be estimated as

$$N_{\rm tot,opt} \sim \frac{\mathcal{F}_{\rm opt}}{h\nu_{\rm opt}} \sim 10^6 {\rm cm}^{-2}, \quad (18)$$

where $\mathcal{F}_{\rm opt}$ is the fluence of the prompt optical emission.

For Fermi, the detectable number of the forward shock EIC radiation can be estimated as

$$N_{\rm det,f} \sim \tau_{\rm f} N_{\rm tot,opt} S_{\rm det} \sim 30. \quad (19)$$

The typical energy of these forward shock EIC photons is

$$h\nu_{\rm EIC,f} \sim 2\min\{\gamma_{\rm c,f}^2, \gamma_{\rm m,f}^2\} h\nu_{\rm opt} \sim 10 \ {\rm GeV}, \quad (20)$$

where $\gamma_{\rm c,f} \sim 10^5 \Gamma_{2.8}^3 R_{17.7} L_{\rm opt,51}^{-1}$ and $\gamma_{\rm m,f} \sim 4\times10^4 \Gamma_{2.8}$.

The Compton parameter $Y_{\rm EIC,f} \sim \gamma_{\rm m,f}^2 \tau_{\rm f} \sim 10$. As the emitted energy of the optical photons was 3×10^{52}ergs (isotropic), the total energy of the EIC photons by forward shocked electrons is $\sim 3\times10^{53}$ergs.

In the rest frame of the forward shock, the seed optical photons have a typical energy $\sim \gamma_e h\nu_{\rm opt}/\Gamma < m_e c^2$ for $\gamma_e < 10^8 \Gamma_{2.8} (h\nu_{\rm opt}/2{\rm eV})^{-1}$. So the EIC scattering in the forward shock front is well in the Thompson regime. The resulting spectrum for $\nu < \nu_{\rm EIC,f} < 1$ TeV is expected to be not steeper than $F_\nu \propto \nu^{-p_{\rm n}/2} \sim \nu^{-1.2}$. On the other hand, the absorption depth for a 30 GeV photons from a redshift $z \sim 1$ is only about 1 (Stecker, Malkan & Scully 2006). So we expect that, if Fermi worked at that moment, it could have detected some photons as energetic as ~ 30 GeV.

Though very bright optical flashes from GRBs are very rare, a few such events are still possible during Fermi's 10 years of operation. Since the EIC component from the forward shock region can give rise to a significant detection for a Fermi-like satellite, here we use the numerical code by Fan et al. (2008) to a more detailed estimate. For simplicity, we approximate the prompt optical emission flux by $F = 10^{-7}(t/10)^6$ erg s^{-1} cm^{-2} for $t < 10$ sec, a constant plateau lasting till $t \sim 60$ sec, and $F = 0$ afterward. The optical spectrum is set as a typical Band function (Band et al. 1993), for which (the break energy, the low energy spectral index, the high energy spectral index) are taken as (2 eV, -1, -2.25), respectively. Notice that it is also a lower limit, as we take the V band as the peak. As shown in Fig. 2, the forward shock EIC emission lasts about twice that of the prompt emission. This is because the duration of the high-energy emission is affected by the spherical curvature of the blast wave (Beloborodov 2005) and is further extended by the highly anisotropic radiation of the up-scattered photons (Fan & Piran 2006; Wang & Mészáros 2006). We also find out that the total energy of the EIC emission is about 10 times that of the prompt optical emission, consistent with our analytical estimate.

2.3 The late GeV-TeV emission of the external forward shock

The high energy emission of the external forward shock has been extensively discussed in literature since 1994 (Mészáros & Rees 1994; Dermer, Chiang & Mitman 2000; Sari & Esin 2001; Wang, Dai & Lu 2001; Zhang & Mészáros 2001; Fan et al. 2008). GRB 080319B is distinguished from most bursts by its huge $E_{\rm k,n}$ and by the large contrast between $\epsilon_{\rm n,e}$ and $\epsilon_{\rm n,B}$, both indicating a very strong high energy radiation component.

In the very early afterglow phase ($t \leqslant 60$ s), the Lorentz factor of the forward shock is almost a constant. The typical Lorentz factor of the shocked electrons is $\gamma_{\rm m} \sim 4\times10^4 \epsilon_{\rm e,n,-1} \Gamma_{2.8}$.

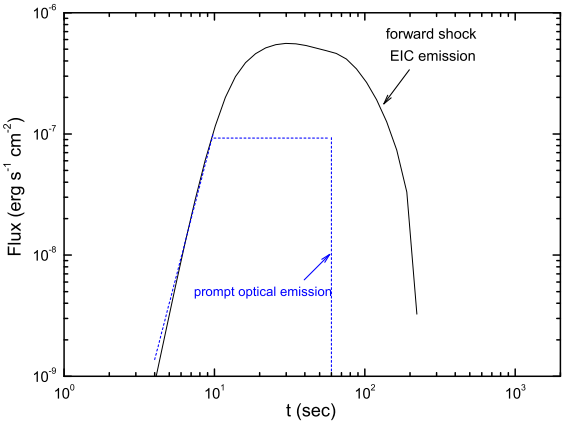

Figure 2. The numerical light curve of GRB 080319B forward shock EIC emission, and the prompt optical prototype is also shown.

After that, the forward shock forms a self-similar profile and its Lorentz factor can be estimated as

$$\Gamma \sim 310(1+z)^{1/4} E_{\rm k,n,55.5}^{1/4} A_{\star,-2}^{-1/4} t_3^{-1/4}. \quad (21)$$

The typical Lorentz factor of the shocked electrons is

$$\gamma_{\rm m} \sim 2\times10^4 (1+z)^{1/4} \epsilon_{\rm e,n,-1} E_{\rm k,n,55.5}^{1/4} A_{\star,-2}^{-1/4} t_3^{-1/4}. \quad (22)$$

At this stage, the forward shock is in the slow cooling phase (Racusin et al. 2008), and $\nu_{\rm m} < \nu_{\rm X} < \nu_{\rm BAT} < \nu_{\rm c}$, where $\nu_{\rm BAT} \sim 10^{20}$ Hz is the frequency of the BAT detector onboard *Swift* satellite and ν_c is the cooling frequency [5]. On the other hand, $\gamma m_e c^2/\gamma_m \sim m_e c^2/100 \sim 10^{18}{\rm Hz} < \nu_c$, implying that the SSC emission of the electrons with a Lorentz factor $\sim \gamma_c$ is in extreme Klein-Nishina regime and it is effectively suppressed. So we expect that the SSC emission will peak at an energy

$$\begin{aligned} h\nu_{\rm p}^{\rm SSC} &\sim \Gamma\gamma_m m_e c^2 \\ &\sim 2.3(\frac{1+z}{2})^{\frac{1}{2}} \epsilon_{e,-1} E_{\rm k,n,55.5}^{1/2} A_{\star,-2}^{-1/2} t_3^{-1/2} {\rm TeV}, \end{aligned} \quad (23)$$

for the very early afterglow ($t \leqslant 60$) sec and the late stage respectively. The SSC emission of the forward shock in the very early afterglow phase overlap with the GeV-TeV emission of the internal shocks and is very likely to be outshone. Below we just discuss the SSC emission of the forward shock in the normal decline phase ($t > 60$ sec).

To check our estimate, we calculate numerically with Fan et al.'s code (2008) the forward shock emission spectrum. As shown in Fig.3, the SSC emission peaks at TeV energies, with a fluence $\sim 6\times10^{-6}{\rm erg\,cm^{-2}}$, and an isotropic energy $\sim 3\times10^{52}{\rm erg}$. The detection of the TeV emission is beyond the scope of the Fermi satellite. Ground based Cherenkov telescopes, like MAGIC and H.E.S.S, may be suitable to detect these energetic signals. However,

[5] For $\nu > \nu_{\rm c}$, the synchrotron radiation spectrum is $\propto \nu^{-p_{\rm n}/2}$. On the other hand, the maximum synchrotron radiation frequency $h\nu_{\rm M} \sim 30\Gamma/(1+z)$ MeV (Cheng & Wei 1996) is up to a few GeV for $\Gamma \geqslant 300$. It is straightforward to show that the fluence of the high energy afterglow emission in the energy range of LAT is in order of 10^{-5} erg cm^{-2}, comparable to the fluence of the soft X-ray/γ-ray afterglow emission. Such a conclusion is almost independent of the afterglow models.

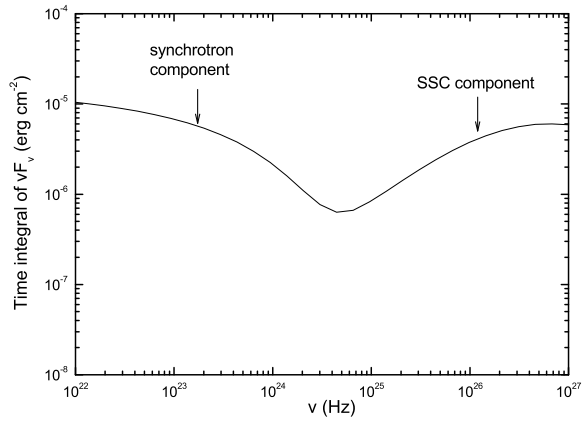

Figure 3. The integral of νF_ν, including the synchrotron + SSC components, in the time interval 60 sec − 2000 sec.

before reaching us, these TeV photons would have been absorbed by the infrared background photons, and such emission could be seen only from rare very nearby sources.

We find in Fig.3 that for a Fermi-like satellite the MeV-GeV synchrotron radiation of the forward shock may give rise to a detectable singal. In our calculation, we take a maximal Lorentz factor of the shocked electrons $\gamma_{\rm M} \sim 4\times10^7 B^{-1/2}$ (Cheng & Wei 1996), where B is the magnetic field generated in the shock front. This leads to the synchrotron GeV cutoff (see Fig.3). As a numerical example, following Fan et al. (2008), we take a real effective area of LAT and integrate the spectrum over the frequencies to estimate the number of detectable photons. For this particular example, the LAT onboard Fermi can detect ~ 400 (>20 MeV), ~ 20 (>1 GeV), and ~ 0.1 (>100 GeV, without the correction due to the absorption by the infrared background photons) high energy photons. It is very interesting to note that these signals are comparable to what LAT has seen in GRB 080916C (Omodei 2008).

3 ORIGINS OF GEV EMISSION OF SOME RECENT GRBS

Recently high energy emission has been detected by AGILE: GRB 080514B (Giuliani et al. 2008), and by Fermi: GRB 080825C (Bouvier et al. 2008), GRB 080916C (Tajima et al. 2008) and GRB 081024B (Omodei et al. 2008). We can apply the above considerations for GRB 080319B to all these bursts, though the very early afterglow data are unavailable and the constraints on the model are not very tight.

GRB 080514B: the burst light curve shows a multi-peaked structure with a duration of $\sim$ 7s (Golenetskii et al. 2008a). The high energy emission lasted about 2 times longer than the MeV emission and the most intense high energy emission arrived at $\sim$ 10 sec after the trigger (Giuliani et al. 2008). We interpret such an intense high energy flash as the EIC emission in the reverse shock region. In this case, some seed photons (the prompt MeV emission) are upscattered by the reverse shock electrons and are boosted to an energy $\lesssim$ 1 GeV (Beloborodov 2005; Fan, Zhang & Wei 2005). The main advantage of this model is that the duration of the high energy emission is longer than that of the prompt soft γ-ray emission by a factor of 2, consistent with the observation. There are also 2 high energy photons detected at $\sim$ 26 s. They may be the synchrotron or SSC emission of the forward shock. The possibility that they are the SSC emission of an underlying X-ray flare (Wei, Yan & Fan 2006; Wang, Li & Mészáros 2006; Galli & Guetta 2008; Fan et al. 2008) cannot be ruled out. The lack of the simultaneous XRT observation makes it difficult to draw further conclusion.

GRB 080916C was a long burst with a duration $\sim$ 60s. The time averaged spectrum, from 8 keV up to 30 MeV, of the main emission is best fitted by a Band function with $E_{\rm p} = 424 \pm 24$keV, $\alpha = -0.91 \pm 0.02$, and $\beta = -2.08 \pm 0.06$. The fluence (8 keV − 30 MeV) is $1.9\times10^{-4}{\rm erg/cm^2}$ (van der Horst & Goldstein 2008, Swift) (slightly different in Konus-Wind observation, Golenetskii et al. 2008a). More than 10 photons are observed above 1 GeV during the prompt phase (Tajima et al. 2008) and the high energy emission lasted longer than the soft $\gamma-$rays (Omodei 2008). This is a very bright burst with a hard spectrum. A simple extension of the keV−MeV spectrum to higher energy range gives $N(30{\rm MeV}-1{\rm GeV}) \sim 700$, $N(1-10{\rm GeV}) \sim 100$ and $N(>10{\rm GeV}) \sim 9$ by LAT (on-axis case), enough to match the observation (Tajima et al. 2008; Omodei 2008). This fact suggests that the synchrotron radiation of the internal shocks plays an important role in producing high energy prompt emission.

On the other hand, the detection of >10 GeV prompt emission gives a tight constraint on the initial bulk Lorentz factor of the GRB outflow, i.e. (Lithiwick & Sari 2001; Fan & Piran 2008),

$$\Gamma_{\rm i} > 400(\frac{h\nu_{\rm cut}}{10{\rm GeV}})^{\frac{p}{2(p+4)}} L_{\gamma,52}^{\frac{1}{p+4}} \delta t_{-2}^{-\frac{1}{p+4}}.$$

Using the maximal synchrotron radiation frequency of the shocks $h\nu_{\rm M} \approx 30\Gamma/(1+z)$ MeV, we find that if the high energy emission up to ~ 10 GeV is attributed to the synchrotron radiation of internal shocks, the initial Lorentz factor should satisfy:

$$\Gamma_{\rm i} \geqslant 330(1+z)\frac{h\nu_{\rm cut}}{10\ {\rm GeV}}.$$

The internal shock synchrotron radiation cannot account for the delayed high energy emission (Omodei 2008). The possible mechanisms that can produce this emission are (i) the EIC emission from the reverse-forward shock regions, (ii) the SSC emission of the forward shock and (iii) SSC emission of the weak internal shocks powering an extended X-ray emission component that is below the threshold of GBM.

GRB 081024B was a short burst with a duration $\sim 0.4-0.8$s (Connaughton et al. 2008; Hanabata et al. 2008). The LAT saw the emission from this source up to 3 GeV, in the first 5 seconds after the trigger. Here we consider two possible interpretations. One is that the delayed emission is the SSC component of an extended/prompt soft X-ray emission. Following Fan & Piran (2008; see their eqs.(47-49)), the typical frequency of the internal shock SSC emission can be estimated as

$$h\nu_{\rm m}^{\rm ssc} \sim 75\ {\rm MeV}\ (E_{\rm p}/1\ {\rm keV})^2 R_{\rm int,13} L_{\rm X,49}^{-1/2}(1+Y_{\rm ssc})^{1/2},$$

where $R_{\rm int}$ is the radius of the continued but weak internal shocks that power the underlying prompt X-ray emission with a luminosity $L_{\rm X}$, and $Y_{\rm ssc}$ is the SSC parameter of the internal shocks. This model requires a unmagnetized outflow launched by the continued activity of the central engine, in contradiction with most models

Table 1. The expected emission of high energy photons from different origins for GRB 080319B, which should be detectable by LAT onboard Fermi satellite.

Seeds	region for electrons	duration (s)	typical photon energy (GeV)	detectable photons
γ-rays	prompt opt	~ 60	$\gtrsim 30$	$\leqslant 100$
opt	prompt γ-ray	~ 60	~ 15	~ 240 †
γ-rays	reverse shock	$\sim 10^2$	~ 13	~ 3
opt	forward shock	$\sim 10^2$	~ 10	~ 30
afterglow	-	$\sim 10^3$	0.01-0.1	~ 400
afterglow	external shock	$\sim 10^3$	$\sim 10^3$	~ 0.04 ‡

†Possibly alternates with the the first case.
‡Supposing an instrument with effect area $10^4 \mathrm{cm}^2$ and without considering the absorption on the way to the observer.

proposed so far (see Zhang 2006 for a review). If confirmed, a stringent constraint on the nature of the extended emission following short GRBs will be established. So, in principle, the cooperation of *Swift* and Fermi satellite can reveal the nature of the late outflow powering the extended emission. The other possible origin of the delayed high energy emission is the SSC emission of the forward shock. It is straightforward to show that the outflow with an initial Lorentz factor $\Gamma_{\rm i} \sim 400$ gets decelerated in the interstellar medium with a number density $\sim 1\ \mathrm{cm}^{-3}$ in ~ 5 sec. The typical SSC emission frequency of the forward shock can be estimated as (Sari & Esin 2001; Fan & Piran 2008)

$$h\nu_{\rm m}^{\rm ssc} \sim 25\ {\rm GeV}\ \epsilon_{e,-1}^{4}\epsilon_{\rm B,-2}^{1/2}\left[\frac{13(p-2)}{3(p-1)}\right]^4 E_{\rm k,51}^{3/4}t_1^{-9/4}.$$

One may be able to distinguish between the above two scenarios by analyzing the spectrum. If the delayed high energy emission is the SSC component of extended but weak internal shocks, the $0.1-3$ GeV spectrum is expected to be steeper than ν^{-1}. If the delayed high energy emission is the SSC component of external forward shock, the $0.1-3$ GeV spectrum is expected to be $\nu^{-1/2}$ unless $p \sim 2$. The forward shock synchrotron radiation can also give rise to GeV emission. It is, however, difficult to say more concerning this possibility because the early afterglow physics of short GRBs is still poorly understood.

4 CONCLUSIONS AND DISCUSSIONS

High-energy emission provides a new window into prompt emission/afterglow physics and can provide an independent test of models. Motivated by this, we calculate the possible high-energy prompt/afterglow emission in GRB 080319B that was distinguished by a naked-eye optical flash and by an unusual strong early X-ray afterglow. Two possible GeV-TeV emission components may be related to the naked-eye optical flash. The first is the Inverse Compton scattering of the prompt optical photons by electrons producing the soft γ-rays. The second is the very early EIC emission from the forward shock region when the prompt optical emission overlaps the shock front. The difference is their duration. The former is expected to be simultaneous with the prompt soft γ-ray emission while the latter lasts longer (see Fig.2). The synchrotron radiation of the forward shock can give rise to a significant detection, too (see Tab. 1 for a summary). This component may be more common than the two that depend on a strong optical flash as which is quite rare. The detection prospect of the forward shock synchrotron radiation by LAT is fairly good. For the *Swift* GRBs detected so far, GRBs 060105, 061007, 070419B and 080721 have a $0.3-10$ keV flux $\sim 10^{-8}\ {\rm erg\,s^{-1}\,cm^{-2}}$ at $t \sim 100$ s after the trigger (http://www.swift.ac.uk/xrt_curves/; Evans et al. 2007). Though about one order of magnitude lower than that of GRB 080319B, they are strong enough to produce a GeV synchrotron emission detectable by LAT as long as the synchrotron spectrum can indeed extend to an energy $\sim 30\Gamma/(1+z)\ {\rm MeV}$. The forward shock SSC emission of these very bright events may be best suitable for the ground-based Cherenkov telescopes, like MAGIC or H.E.S.S.

In section 3, we discussed the physical origin of the high energy emission of GRB 080514B, GRB 080916C and GRB 081024B. We find that these detections can be well understood by the synchrotron and inverse Compton radiation of the internal shocks or external shocks. For example, the delayed sub-GeV flash detected in GRB 080514B may be the EIC emission from the reverse shock region and the prompt GeV-emission of GRB 080916C may be dominated by the synchrotron radiation of the internal shocks. The "long lasting" high energy emission detection in the short burst GRB 081024B may be attributed to the SSC emission of the decelerated forward shock or the internal shocks powering an extended X-ray component that is below the threshold of GBM.

Finally we focus on the common feature that the high energy emission usually lasts longer than the prompt soft γ-rays, as detected in GRB 080514B, GRB 080916C and GRB 081024B. Such a phenomena, peculiar in pre-afterglow era, can be well understood now: (1) The synchrotron and the SSC emission of the long lasting forward external shock can contribute to the high energy emission significantly. (2) The GRB central engines usually do not turn off abruptly. The SSC emission of the continued but weak internal shocks may peak at GeV energies. (3) If a (mildly) relativistic reverse shock formed, the prompt optical/X-ray/γ-ray photons overlap the external shock fronts tightly and cool the accelerated electrons effectively. This process will produce a GeV emission component with a duration about twice that of the prompt photons. For a sub-relativistic reverse shock, the prompt soft $\gamma-$ray photons exceed the external shock fronts quickly. Its effect on cooling the reverse/forward shock electrons can be ignored. However in such a case the electrons/protons accelerated in reverse shock contain just $\sim 10\%$ of the total energy of the GRB ejecta (Nakar & Piran 2004; Mimica 2008) and cannot play an important role in producing high energy emission. (4) The EIC in the late afterglow phase caused by X-ray flares can also give rise to GeV emission. However the luminosity is lowered since its duration has been significantly extended. Usually LAT is unable to catch such a weak signal.

ACKNOWLEDGMENTS

YZF thanks Bing Zhang and Daming Wei for discussions. This work is supported in part by the Israel Science Foundation (for TP), a grant from the Danish National Science Foundation, a special grant of Chinese Academy of Sciences, National basic research program of China grant 2009CB824800, and the National Natural Science Foundation of China under the grants 10673034 (for YZF) and 10703002 (for YCZ).

REFERENCES

Band D. et al., 1993, ApJ, 413, 281
Beloborodov A. M., 2005, ApJ, 618, L13
Blandford R. D., McKee C. F., 1976, Phys. Fluids., 19, 1130
Bloom J. S., et al., 2008, ApJ submitted (arXiv:0803.3215)
Bouvier A., et al., 2008, GCN circular, 8183
Cheng K. S., Wei D. M., 1996, MNRAS, 283, L133
Chevalier R. A., Li Z. Y., 2000, ApJ, 536, 195
Connaughton V., et al., 2008, GCN circular, 8408
Cwiok M., et al., 2008, GCN circular, 7445
Dai Z. G., Lu T., 1998, MNRAS, 298, 87
Dermer C. D., Chiang J., Mitman K. E., 2000, ApJ, 537, 785
Evans P. A., et al., 2007, A&A, 469, 379
Fan Y. Z., Piran T., 2006, MNRAS, 370, L24
Fan Y. Z., Piran T., 2008, Front. Phys. Chin., 3, 306 (arXiv:0805.2221)
Fan Y. Z., Piran T., Narayan R., Wei D. M., 2008, MNRAS, 384, 1483
Fan Y. Z., Zhang B., Wei D. M., 2005, ApJ, 629, 334
Galli A., Guetta D. A., 2008, A&A, 480, 5
Giuliani A., et al., 2008, A&A, 491, L25
Golenetskii, S., Aptekar, R., Mazets, E., Pal'shin, B., Frederiks, D., Cline, T., 2008, GCN circualr, 7482
Golenetskii S., et al., 2008, GCN circular 7751
Golenetskii S., et al., 2008b, GCN circular 8258
González M. M., Dingus B. L., Kaneko Y., Preeze R. D., Dermer C. D., Briggs M. S., 2003, Nature, 424, 749
Hanabata Y., et al., GCN circular, 8444
Hurley K., Dingus B. L., Mukherjee R., et al., 1994, Nature, 372, 652
Jin Z. P., Fan Y. Z., 2007, MNRAS, 378, 1043
Jin Z. P., Yan T., Fan Y. Z., Wei D. M. 2007, ApJ, 656, L57
Karpov S., et al., 2008, GCN Circular 7502
Kumar P., Panaitescu, A., 2008, MNRAS, 391, L19
Margutti R., Guidorzi C.,Chincarini G., Pasotti F.,Covino S., Mao J., 2008, arXiv:0809.0189
Marisaldi M., et al., 2008, GCN circular, 7457
Mészáros P., 2002, ARA&A, 40, 137
Mészáros P., Rees M. J., 1994, MNRAS, 269, L41
Mimica P., Giannios D., Aloy M. A., 2008, A&A, in press (arXiv:0810.2961)
Nakar E., Piran T., 2004, MNRAS, 353, 647
Omodei N., et al., 2008, GCN circular, 8407
Omodei N., 2008, talk given at the "6th Workshop on Science with the New Generation of High Energy Gamma-ray Experiments" (http://glast.pi.infn.it/presentations/081008_GRB_Abano.ppt)
Panaitescu A., Kumar P., 2001, ApJ, 554, 667
Piran T., 2004, Rev. Mod. Phys., 76, 1143
Piran T., Sari R., Zou Y. C., 2008, MNRAS, in press (arXiv:0807.3954)
Racusin J., et al., 2008b, GCN circular, 7427
Racusin J. L., et al., 2008, Nature, 455, 183
Sari, R., Esin, A., 2001, ApJ, 548, 787
Sari R., Piran T., Narayan R., 1998, ApJ, 497, L17
Stecker F. W., Malkan, M. A., Scully S. T., Astrophys. J., 2006, 648, 774
Tajima H., et al., 2008, GCN circular, 8246
van der Horst A., Goldstein A., 2008, GCN circular, 8278
Vreeswijk P. M., et al., 2008, GCN circular, 7444
Wang X. Y., Dai Z. G. & Lu T., 2001, ApJ, 556, 1010
Wang X. Y., Li Z., Mészáros P., 2006, ApJ, 641, L89
Wang X. Y., Mészáros P., 2006, ApJ, 643, L95
Wei D. M., Yan T., Fan Y. Z., 2006, ApJ, 636, L69
Wu X. F., et al., 2008, ApJ, to be submitted
Zhang B., 2006, AIPC, 838, 392
Zhang B., 2007, ChJAA, 7, 1
Zhang B., Mészáros P., 2001, ApJ, 559, 110
Zou Y. C., Wu X. F., Dai Z. G., 2005, MNRAS, 363, 93
Zou Y. C., Piran T., Sari R., 2008, in preperation